NEIGHBOUR LOCAL VARIABILITY FOR MULTI-FOCUS IMAGES FUSION

Ias Sri Wahyuni[1] and Rachid Sabre[2]

[1]Universitas Gunadarma, Jl. Margonda Raya No. 100 Depok 16424, Indonesia
[2]Laboratory Biogéosciences CNRS, University of Burgundy/Agrosup Dijon, France

ABSTRACT

The goal of multi-focus image fusion is to integrate images with different focus objects in order to obtain a single image with all focus objects. In this paper, we give a new method based on neighbour local variability (NLV) to fuse multi-focus images. At each pixel, the method uses the local variability calculated from the quadratic difference between the value of the pixel and the value of all pixels in its neighbourhood. It expresses the behaviour of the pixel with respect to its neighbours. The variability preserves the edge function because it detects the sharp intensity of the image. The proposed fusion of each pixel consists of weighting each pixel by the exponential of its local variability. The quality of this fusion depends on the size of the neighbourhood region considered. The size depends on the variance and the size of the blur filter. We start by modelling the value of the neighbourhood region size as a function of the variance and the size of the blur filter. We compare our method to other methods given in the literature. We show that our method gives a better result.

KEYWORDS

Neighbour Local Variability; Multi-focus image fusion; Root Mean Square Error (RMSE)

1. INTRODUCTION

The limitation of the depth of field of optical lenses often causes difficulty in capturing an image containing all objects in focus on the scene. Only objects in depth of field are sharp, while other objects are out of focus. Merging multi-focus images is the solution to this problem. There are different approaches that have been carried out in the literature. These approaches can be separated into two kinds: the spatial domain method and the multi-scale fusion method. The spatial domain fusion method is performed directly on the source images. The techniques of the spatial domain directly consider the pixels of the image. We quote some methods of fusion of the spatial domain approaches: the mean, the principal component analysis (PCA) [1], the rule of maximal selection, the methods bilateral gradient based [2] and guided image filter (GIF) method [3] and maximum selection rule. We relate to the spatial domain approaches the fact that they produce a spatial distortion in the merged image. Spatial distortion can be handled very well by multiscale approaches to image fusion. The merging process in multi-scale merging methods is done on the source images after their decomposition into several scales. we cite some examples of these methods: The discrete wavelet transform (DWT) [4] - [9], fusion of images of the Laplacian pyramid [10] - [17], discrete cosine transform with variance calculation (DCT + var) [18], method based on salience detection (SD) [19] are examples of image fusion techniques under transformation domain. The objective of this work is to propose a multi-focus image fusion at the pixel level based on the neighboring local variability (NLV). It consists in calculating for each pixel the quadratic distance which separates it from the other pixels belonging to its neighborhood. It expresses the behavior of the pixel with respect to all the pixels belonging to its

neighborhood. The variability preserves the edge function because it detects the sharp intensity of the image. The fusion of each pixel is given by a linear model of the values of the pixel in each image hanging by the exponential of its local variability.

The precision of this fusion depends on the width of the region of pixels considered in the neighbourhood. To determine this optimal width, we minimize the RMSE error. We propose a model giving this width as a function of the variance and the size of the blur filter.

A comparative study of our method with other existing methods in the literature (DWT and LP-DWT), it was carried out and showed that our method gave the best result using the mean squared error (RMSE).

This paper is organized as follows: The second section reveals the stages of the process of fusing the proposed method and a model giving the size of the neighbourhood. In section 3, we studied the experimental results and compared our method to some recent methods. Section 4 gives the conclusion of this work. In section 5, we give mathematical details to show the property of local variability..

2. NEIGHBORING LOCAL VARIABILITY METHOD

Let be the fusion of two images, I1 and I2 that respectively have blurred parts B1 and B2. These images have the same size: N1 x N2 where B1 and B2 are disjoint. The idea of the NLV merge method is to add the pixel values of the two images weighted by the local variability of each image. This local variability at (x, y) is calculated from the exponential of average of the square difference between the value of the pixel (x, y) and the value of its neighbors. The NLV at is defined as follows:

$$v_{a,k}(x,y) = \sqrt{\frac{1}{R}\sum_{m=-a}^{a}\sum_{n=-a}^{a}\left|I_k(x,y) - I'_k(x+m,y+n)\right|^2} \quad (1)$$

where k is the index of k^{th} source image (k = 1, 2), a is the size of neighborhood

$$I_k^{'}\left(x+m,y+n\right) = \begin{cases} I_k(x+m,y+n), \ if \ 1 \le x+m \le N_1 \ and \ 1 \le y+n \le N_2 \\ I_k(x,y), \ otherwise \end{cases},$$

$$R = (2a+1)^2 - card(S),$$

$$S = \left\{(m,n) \in \left(\left[-a,a\right]^2 - \{(0,0)\}\right) \middle| I_k^{'}\left(x+m,y+n\right) = I_k(x,y)\right\}.$$

In the annex 1,we show that this local variability is small enoughwherethe location is on theblurred area (B_1 or B_2).

In this work, we give a novel fusion method where each pixel of each image is weighting by exponential of neighbour local variability. We calculate the neighbour local variabilityfrom the quadratic difference between the value of the pixel and the all pixel values of its neighbours. The idea came from the fact that the variation of the value in blurred region is smaller than the variation of the value in focused region. We used the neighbour, with the size "a", of a pixel defined as follows:

$(x+i, y+j)$ where $i = -a, -a+1, \ldots, a-1, a$ and $j = -a, -a+1, \ldots, a-1, a$.

For example, the neighbor with the small size ("a" = 1) contains: $(x-1,y-1)$, $(x-1,y)$, $(x-1,y+1)$, $(x,y-1)$, $(x,y+1)$, $(x+1,y-1)$, $(x+1,y)$, $(x+1,y+1)$.

	(x-1, y-1)	(x-1,y)	(x-1,y+1)	
	(x,y-1)	(x,y)	(x,y+1)	
	(x+1,y-1)	(x+1,y)	(x+1,y+1)	

Fig. 2. Pixel at (x,y) within its neighborhood, a = 1.

The fusion with size "a"follows the steps:

Consider M original source images, I_1, ..., I_M, with different focus and same size$(N_1 \text{x} N_2)$.
Step 1: For each pixel of each image, we calculated the neighbor local variability (NLV) of every source image, $v_{a,k}(x,y)$ defined in (1).

Step 2: The proposed fusion for the pixel (x,y) is $F(x,y)$ calculated by the following model:

$$F(x,y) = \frac{\sum_{k=1}^{M} \exp\left(v_{a,k}(x,y)\right) I_k(x,y)}{\sum_{i=1}^{M} \exp\left(v_{a,k}(x,y)\right)} \quad (2)$$

We remark that method depends on the size "a". To determine the value of "a" , we find the value minimizing the Root Mean Square Error (RMSE), where RMSE is defined in section 3. For that, we showed that the value of "a" depends on the blurred area.

The choice of the size of the neighborhood "a" used in NLV method depends on variance (v) and the size(s) of the blurring filter. Our problem is to have a model that gives the value of the "a" according to the "v" and "s"; we take a sample of 1000 images that we blurred using Gaussian filter with different values of v and s (v=1,2,3,...,35 and s=1,2,3,...,20).

After that, for each image we blurred with parameters "v" and "s", we applied our fusion method with different values of "a"("a=1,2,...,17")and determined the value of "a" that gives the minimum RMSE, denoted by $a_I(v,s)$. Then, we took the mean of the $a_I(v,s)$ for 1000 images, denoted $a(v,s)$, because the coefficient of variation is smaller than 0,1.

Firstly, we have studied the variation of "a" in according to variance "v" for each fixed size of blurring filter "s". We noted that this variation is logarithmic. For example, "s=8" on Fig. 4.By using nonlinear regression, we obtained the model:

$$\text{a}= 2.1096 \ln v + 2.8689.$$

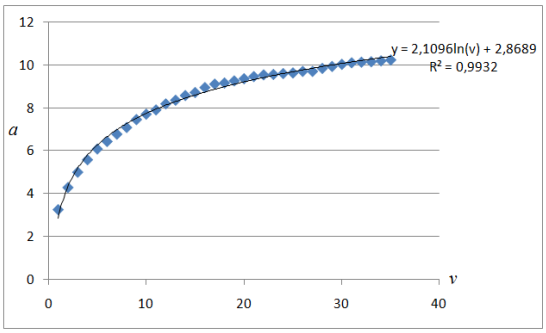

Fig. 4. Graph between "a" and variance of blurring filter where "s"=8.

In general, the model is:

$$a = c_1(s)\ln v + c_2(s) \quad (3)$$

where the c_1 and c_2 are functions that depend on "*s*". The graphs that describe c_1 and c_2, respectively, are revealed in Fig. 5. and Fig. 6.

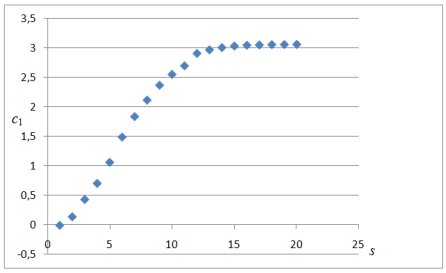

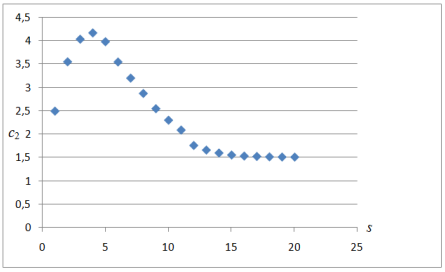

Fig. 5. graph of $c_1(s)$ Fig. 6. graph of $c_2(s)$.

By giving a model of c_1 and a model of c_2 and introducing these models in (3), we get the general following model:

$$a(v,s) = \frac{3.0348761}{1+29.0909139\exp(-0.5324955s)}\ln(v) + 0.434\left(\frac{75.062269}{1.225175s}\right)\exp\left(-0.5\left(\frac{\log(s)-2.655551}{1.225175}\right)^2\right) \quad (4)$$

As "*a"* is integer, we have two choices of *a*. *It* is either the floor of $a(v,s)$, denoted by $\lfloor a(v,s) \rfloor$ or the ceiling of *a*(v,s) , denoted by $\lceil a(v,s) \rceil$ where $\lfloor x \rfloor = \min\{n \in \square \mid n \geq x\}$ and $\lceil x \rceil = \max\{m \in \square \mid m \leq x\}$. Since the RMSE values of both "*a*" are very slightlydifferent, then we can choose any "*a*" of them. We use "*a*" = $\lfloor a(v,s) \rfloor$ in the remaining part of this paper.

To validate this model we applied it to 100 images (we generated 100 pairs of multi-focus images with different variance and blur filter size values) and the result is as good as expected. To use this NLV method, you must first estimate the variance and size of the blur filter from the blur image. For this, there are some articles giving the methods to estimate the variance of the blur

filter and the blur detection as in [23] - [27]. subsequently, we developed another method in which we combined the method of the Laplacian pyramid and the NLV method where the Laplacian pyramid was used with NLV as selection rule, denoted LP-NLV.

3. EXPERIMENTAL STUDY

We have applied the NLV method on a dataset of images [26] using Matlab2013a. These images were blurred using a Gaussian filter with many values of variance and size. To simplify the reading of the article, we have presented only two examples in 256x256 format (N1 = N2 = 256). The first “bird” image Fig.1 and the second “bottle” image Fig.2. All images consist of two images with a different focus and a reference image.

We then compare the NLV method to other methods existing in the literature such as: PCA method [1], Discrete Wavelet Transform (DWT) method [6], Laplacian Pyramid LP_PCA [15], LP_DWT [17] and Bilateral gradient (BG) [2].

For that, we used the following the evaluation criteria frequently used:
Root Mean Square Error (RMSE)

RMSE gives the information how the pixel values of fused image F deviate from the reference imageR. RMSE is defined as follows:

$$RMSE = \sqrt{\frac{1}{rc}\sum_{i=1}^{c}\sum_{j=1}^{c}\left[R(x,y)-F(x,y)\right]^2} \qquad (5)$$

where*R* is a reference image, *F* is a fused image,*r*x *c* is the size of the input image, and *x, y* represents to the pixel locations. A smaller value of RMSE shows a good fusion result. If the value of RMSE is equal to zero then it means the fused image is same the reference image.

For two images that are presented in this paper and blurred with variance = 10 and size of blurring filter = 5, the model (5) gives the neighbour size "a" = 5 and "a" = 6. Here, we use "a" = 6 because it results the smaller RMSE compared to "a" = 5 however the RMSE values of "a" = 5 and "a" = 6 are very slightly different.

Blurred image 1

Blurred image 2

Figure1. Fusion by proposed method NLV

We have found that the NLV method better fusion compared to other methods, see Fig.1.

Table 1. Performance evaluation of image 'bird'

	PCA	DWT	LP-DWT	LP-PCA	DCT+var	Bilateral gradient	GIF	SD	NLV	LP-NLV
RMSE	6.9205	3.5678	1.5190	1.4681	2.6860	8.8378	2.2792	10.4547	**0.5466**	0.8431

The table 1 gives the values of RMSE calculated for ten methods. As we can see on the Table 1 for image 'bird': the smallest RMSE is given by NLV method, the second smallest is LP-NLV, the third is LP-PCA,. NLV method is the best method among the above methods and LP-NLV is better than LP-PCA and LP-DWT.

Blurred image1 Blurred image2

Figure2. Fusion by proposed method (NLV)

We have found that the NLV method performs better compared to other methods, see Fig.2.

To confirm our visually result, we calculated the evaluation metrics: RMSE for ten methods see Table 2. We can classify these methods from the smaller value of RMSE. The smallest value is NLV, the second smallest is LP-NLV and the third smallest is LP-PCA.

Table 2. Performance evaluation of images of 'the bottle'

	PCA	DWT	LP-DWT	LP-PCA	DCT+var	Bilateral gradient	GIF	SD	NLV	LP-NLV
RMSE	15.005	5.384	2.528	2.485	2.642	20.380	3.681	16.919	**0.902**	1.584

According to the evaluation measure RMSE, the Table 3 gives the mean and standard deviation of RMSE for the considered methods applied on 150 images.

Table 3. Statistic parameters of the sample (150 images)

Methods	PCA	DWT	LP_DWT	LP_PCA	DCT_var	BG	NLV	LP_NLV
Mean	8,713	4,194	2,049	1,995	2,839	11,044	0,591	1,344
Standard deviation	3,866	1,381	0,756	0,743	1,308	4,859	0,204	0,697
Time of execution by image	7s	5s	7s	7s	6s	6s	5s	7s

Table 3 shows that the proposed method (NLV) has a smaller average of the RMSE. The RMSE histograms for 150 images by different methods (Figures 3, 4, 5, 6, 7, 8 and 9) show for almost all methods that the RMSE values are almost symmetrically centered around the mean value.

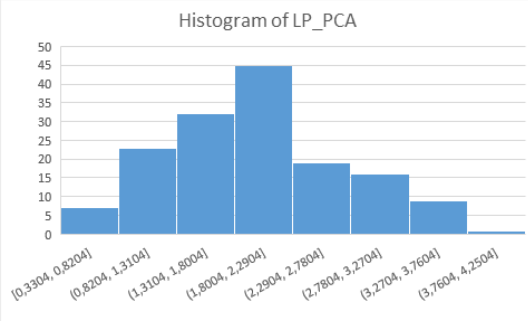

Figure 3. Histogram of PCA method

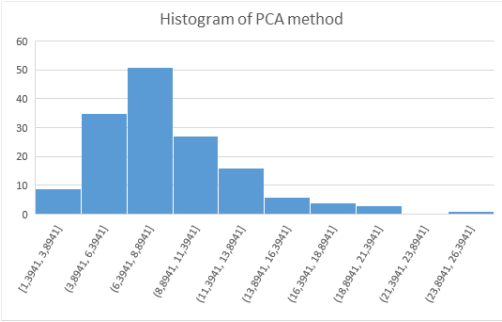

Figure 4. Histogram of LP_PCA method

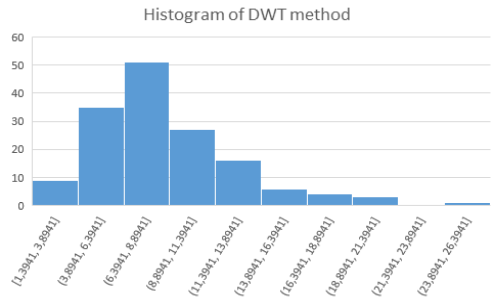

Figure 5. The Histogram of DWT method

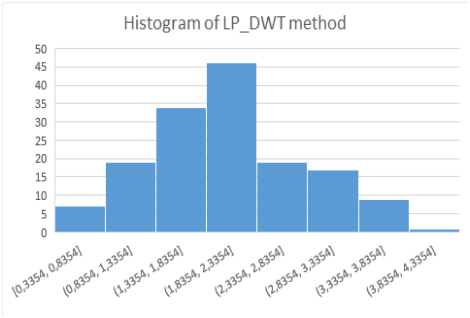

Figure 6. Histogram of LP_DWT method

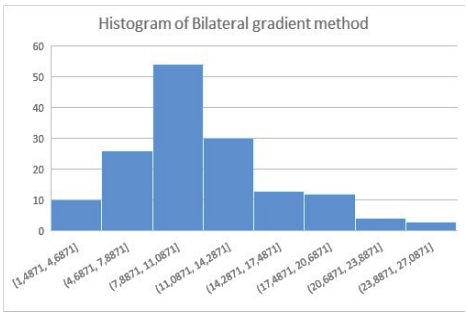

Figure 7. Histogram of Bilateral gradient method

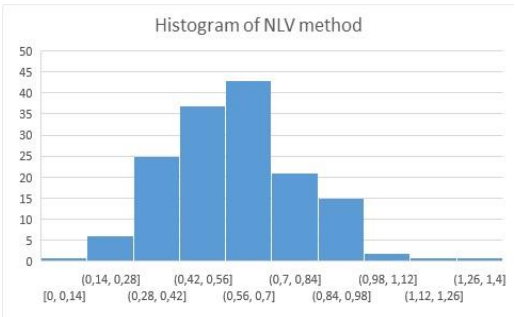

Figure 8. Histogram of NLV method

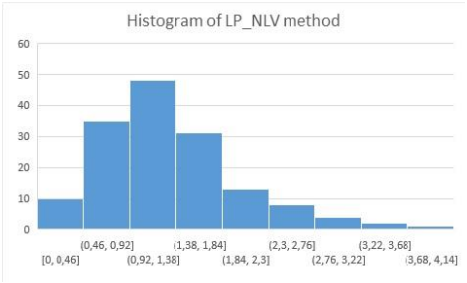

Figure 9. Histogram of LP_NLV method

In order to compare analytically the proposed method to other methods,a study of the Analysis of variance (ANOVA) with dependent samples (dependence by image) is done. The software R gives the following Anova table:

Table 4. Anova table with one factor: method

	Df	Sum Sq	Mean Sq	F value	Pr(>F)
Method	9	25467	2829.6	742	<2e-16 ***
Residuals	1341	5114	3.8		

As Pr(>F) is smaller than 1% , in table 4., the methods are significantly different. Then, the Newman Keuls test is performed for comparing the methods two-by-two and giving groups having significantly the same mean of RMSE. The software R shows the results of the test as follows:

Table 5. Test of Newman Keuls

$groups		
	RMSE	groups
SD	12.6072900	a
BG	11.0447767	b
PCA	8.7139600	c
DWT	4.1941660	d
DCT_var	2.8395233	e
GIF	2.5146353	e
LP_DWT	2.0496413	f
LP_PCA	1.9954953	f
LP_NLV	1.3446913	g
NLV	0.5921593	h

From table 5, we obtained the methods significantly different except the methods DCT_var and GIF form the group “e” and the methods LP_DWT and LP_PCA form the group “f”.

The proposed method NLV in group “h” has a smaller mean (0.5921593) and significantly different of the all methods. We conclude that the proposed method gives the better result than other methods.

4. CONCLUSION

In this paper we propose an image fusion method based on local neighbour variability (NLV). This method has been described in detail. Applying this method to 150 images gives a result of significant improvement in both visual and quantitative image fusion compared to other fusion

methods. We used Laplacian pyramid with NLV as selection criterion, LP-NLV. Based on the result of the experiment, we notice that LP-NLV is better than LP-DWT and DWT.

The proposed method has the advantage of taking into account the variability between each pixel and its neighbours. Thus the coefficient of the pixels located in the focused part will be more imposing. This method can be extended to multimodal images used in particular in medicine (scanner, ultrasound, radiography, etc.) to give the presence of certain cancer cells seen in one image and not visible in another image.

1) Drone is considered as a technological means allowing to capture images at different altitudes. It opened up limitless possibilities for improving photography. The captured images can be on the same scene by zooming in on different objects and at different altitudes. It produces several images on the same scene but with different objects in focus.

2) In the food industry to control the quality of some products, cameras have been used to take pictures. Each camera targets one of many objects placed on a conveyor belt to detect an anomaly. To have a photo containing all the objects clearly, we can use the proposed merge method which gives more details.

The perspectives of this work:

- We intend to extend our method to color images because color conveys additional information.
- Encouraged by these results, we plan to extend the NLV method to the fusion of more than two images, taking into account the local variability of each image (intra-variability) and the variability between the images (inter-variability). Inter-variability can detect "abnormal pixels" among images.

REFERENCES

[1] Naidu, V.P.S. and. Raol, J.R. (2008) “Pixel-level Image Fusion using Wavelets and Principal Component Analysis”, Defence Science Journal, Vol. 58, No. 3, pp. 338-352.
[2] Tian, J., Chen, L., Ma, L., Yu, W., (2011) “Multi-focus image fusion using a bilateral gradient-based sharpness criterion”, Optic Communications, 284, pp 80-87.
[3] Zhan, K., Teng, J., Li, Q., Shi, J. (2015) “A novel explicit multi-focus image fusion method”, Journal of Information Hiding and Multimedia Signal Processing, vol. 6, no. 3, pp.600-612.
[4] Mallat, S.G. (1989) “A Theory for multiresolution signal decomposition: The wavelet representation”, IEEE Trans. Pattern Anal. Mach. Intel., 11(7), 674-93.
[5] Pajares, G., Cruz, J.M. (2004) “A Wavelet-Based Image Fusion Tutorial”, Pattern Recognition 37. Science Direct.
[6] Guihong, Q., Dali, Z., Pingfan, Y. (2001) “Medical image fusion by wavelet transform modulus maxima”. Opt. Express 9, pp. 184-190.
[7] Indhumadhi, N., Padmavathi, G., (2011) “Enhanced Image Fusion Algorithm Using Laplacian Pyramid and Spatial Frequency Based Wavelet Algorithm”, International Journal of Soft Computing and Engineering (IJSCE). ISSN: 2231-2307, Vol. 1, Issue 5.
[8] Sabre, R. Wahyuni, I.S, (2020) “Wavelet Decomposition and Alpha Stable”, Signal and Image Processing (SIPIJ), Vol. 11, No. 1. pp. 11-24.
[9] Jinjiang Li , Genji Yuan and Hui Fan (2019) “Multifocus Image Fusion Using Wavelet-Domain-Based Deep CNN”, Computational Intelligence and Neuroscience, Vol. 2019 Article ID 4179397 | https://doi.org/10.1155/2019/4179397
[10] Burt, P.J., Adelson, E.H. (1983) “The Laplacian Pyramid as a Compact Image Code”, IEEE Transactions on communication, Vol.Com-31, No 40.

[11] Burt, P.J. (1984) "The Pyramid as a Structure for Efficient Computation. Multiresolution Image Processing and Analysis", A. Rosenfeld, Ed., Springer-Verlag. New York.
[12] Burt, P.J., Kolezynski, R.J. (1993) "Enhanced Image Capture Through Fusion", in: International Conference on Computer Vision, pp. 173-182.
[13] Wang, W., Chang, F. (2011) "A Multi-focus Image Fusion Method Based on Laplacian Pyramid", Journal of Computers, Vol.6, No 12.
[14] Zhao, P., Liu, G., Hu, C., Hu, and Huang, H. (2013) "Medical image fusion algorithm on the Laplace-PCA". Proc. 2013 Chinese Intelligent Automation Conference, pp. 787-794.
[15] Verma, S. Kaur K.,, Kumar M., R..(2016) "Hybrid image fusion algorithm using Laplacian Pyramid and PCA method", proceeding of the Second International Conference on Information and Communication Technology for Competitive Strategies.
[16] Wahyuni, I.S, Sabre, R. (2019) "Multifocus Image Fusion Using Laplacian Pyramid Technique Based on Alpha Stable Filter", CRASE Vol. 5, No. 2. pp. 58-62.
[17] Wahyuni, I.S, Sabre, R. (2016) "Wavelet Decomposition in Laplacian Pyramid for Image Fusion", International Journal of Signal Processing Systems Vol. 4, No. 1. pp. 37-44.
[18] Haghighat, M.B.A, Aghagolzadeh, A., Seyedarabi, H. (2010) "Real-time fusion of multifocus images for visual sensor networks". Machine vision and image processing (MVIP), 2010 6th Iranian. 2010.
[19] Bavirisetti, D.P., and Dhuli, R.(2016) ''Multi-focus image fusion using multi-scale image decomposition and saliency detection'', Ain Shams Eng. J., to be published. [Online]. Available: http://dx.doi.org/ 10.1016/j.asej.2016.06.011.
[20] Petland, A. (1984) "A new sense for depth of field", IEEE Transactions on Pattern Analysis and Machine Intelligent, Vol. 9, No. 4, pp. 523-531.
[21] Nayar, S.K.(1992) "Shape from Focus System", Proc. of IEEE Conf. Computer Vision and Pattern Recognition, pp. 302-308.
[22] Gonzales, R.C., Woods, R.E. (2002) "Ditigal Image Processing" 2nd edition. Prentice Hall.
[23] Liu,R., Li, Z., Jia, J.(2008) "Image Partial Blur Detection and Classification", Computer Vision and Pattern Recognition, CVPR 2008. IEEE Conference DOI: 10.1109/CVPR.2008.4587465
[24] Aslantas, V. (2007) "A depth estimation algorithm with a single image." Optic Express, Vol. 15, Issue 8. OSA Publishing.
[25] Elder, J.H., Zucker, S.W. (1998) " Local Scale Control for Edge Detection and BlurEstimation." IEEE Transactions on Pattern Analysis and Machine Intelligence,Vol.20, No.7.
[26] www.rawsamples.ch. Accessed: 15 November 2017.
[27] Kumar, A., Paramesran, R., Lim, C. L., and Dass, S.C. (2016) "Tchebichef moment based restoration of Gaussian blurred images". Applied Optics, Vol. 55, Issue 32, pp. 9006-9016.

5. ANNEX 1

Consider, without loss the generality that we have a focus pixel (x, y) in image I_1 and blurred in image I_2 as in Fig. 1.

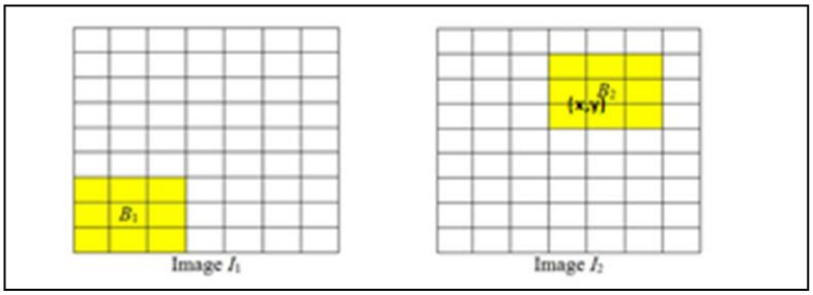

Fig. 1. Two multi-focus images, the yellow part is blurred area and the white part is clear (focus) area.

The neighbor local variability of images I_1 and I_2, respectively is defined in (1) by:

$v_{a,1}(x,y) = \exp\left(\sqrt{\frac{1}{R}r_1(x,y)}\right)$ and $v_{a,2}(x,y) = \exp\left(\sqrt{\frac{1}{R}r_2(x,y)}\right)$ where $r_1(x,y)$and $r_2(x,y)$

can be written as follows:

$$r_1(x,y) = \sum_{m=0}^{2a}\sum_{n=0}^{2a}\left|I_1(x,y) - I_1\big(x+(m-a), y+(n-a)\big)\right|^2 \quad (6)$$

$$r_2(x,y) = \sum_{m=0}^{2a}\sum_{n=0}^{2a}\left|I_2(x,y) - I_2\big(x+(m-a), y+(n-a)\big)\right|^2 \quad (7)$$

Let I_R is the reference image of multi-focus images I_1 and I_2. Moreover, it is shown in [20] and [21] that the blurred image can be seen as the product convolution between the reference image and Gaussian filter:

$$I_1(x,y) = \begin{cases} w_1 * I_R(x,y), & (x,y) \in B_1 \\ I_R(x,y), & (x,y) \notin B_1 \end{cases} \quad I_2(x,y) = \begin{cases} w_2 * I_R(x,y), & (x,y) \in B_2 \\ I_R(x,y), & (x,y) \notin B_2 \end{cases}, \quad (8)$$

where w_1 and w_2 are Gaussian filter defined by:

$$w_1(k,l) = w_1(k,l) = \frac{\exp\left(-\frac{k^2+l^2}{2\sigma_1{}^2}\right)}{\sum_{k=-s_1}^{s_1}\sum_{l=-s_1}^{s_1}\exp\left(-\frac{k^2+l^2}{2\sigma_1{}^2}\right)}, \ (\mathrm{k},\mathrm{l}) \in [-s_1, s_1]^2,$$

$$w_2(k,l) = \frac{\exp\left(-\frac{k^2+l^2}{2\sigma_2{}^2}\right)}{\sum_{k=-s_2}^{s_2}\sum_{l=-s_2}^{s_2}\exp\left(-\frac{k^2+l^2}{2\sigma_2{}^2}\right)}, (k,l) \in [-s_2, s_2]^2$$

The product convolution is defined as follows:

$$w_1 * I_R(x,y) = \sum_{k=-s_1}^{s_1}\sum_{l=-s_1}^{s_1} w_1(k,l) I_R(x-k, y-l), \ w_2 * I_R(x,y) = \sum_{k=-s_2}^{s_2}\sum_{l=-s_2}^{s_2} w_2(k,l) I_R(x-k, y-l),$$

Put $r_1(x,y) = \sum_{m=0}^{2a}\sum_{n=0}^{2a}\left|D^1_{(m,n)}(x,y)\right|^2$ and $r_2(x,y) = \sum_{m=0}^{2a}\sum_{n=0}^{2a}\left|D^2_{(m,n)}(x,y)\right|^2$ (9)

where $D^1_{(m,n)}(x,y) = I_1(x,y) - I_1\big(x+(m-a), y+(n-a)\big)$ (10)

$$D^2_{(m,n)}(x,y) = I_2(x,y) - I_2\left(x+\left(m-a\right), y+\left(n-a\right)\right) \tag{11}$$

Proposition:

The local variability on blurred part is smaller than the local variability on focused part. Let $(x,y) \in B_2$ (the blurred part of I_2) and $(x,y) \notin B_1$ (focus par of I_1), then $\left(r_2(x,y) \le r_1(x,y)\right)$.

Proof:

For that, we use Plancherel theorem:

$$\sum_{m=0}^{2a}\sum_{n=0}^{2a}\left|D^1_{(m,n)}(x,y)\right|^2 = \frac{1}{(2a+1)^2}\sum_{m=0}^{2a}\sum_{n=0}^{2a}\left|\widehat{D}^1_{(n,m)}(x,y)\right|^2 \tag{12}$$

where $\widehat{D}^1_{(n,m)}(x,y)$ is Fourier transform of $D^1_{(m,n)}(x,y)$.

$$\widehat{D}^1_{(n,m)}(x,y) = FT\left[D^1_{(m,n)}(x,y)\right] = FT\left[I_1(x,y) - I_1\left(x+(m-a), y+(n-a)\right)\right] \tag{13}$$

As $(x,y) \in B_2$ therefore $(x,y) \notin B_1$, from (12), equation (13) can be written as follows:

$$\widehat{D}^1_{(n,m)}(x,y) = FT\left[I_R(x,y) - I_R\left(x+(m-a), y+(n-a)\right)\right] \tag{14}$$

and

$$I_2(x,y) = \sum_{k=-s_2}^{s_2}\sum_{l=-s_2}^{s_2} w_2(k,l) * I_R(x-k, y-l) \tag{15}$$

By using the definition of convolution, equation (15) can be written as:

$$I_2(x,y) = \sum_{k=-\infty}^{\infty}\sum_{l=-\infty}^{\infty} w_2(k,l)1_{[-s_2,s_2]^2} I_R(x-k, y-l) \tag{16}$$

and

$$I_2(x,y) = \left(w_2 1_{[-s_2,s_2]^2}\right) * I_R(x,y) \tag{17}$$

where

$$1_{[-s_2,s_2]^2}(k,l) = \begin{cases} 1, & if\ \ (\mathrm{k,l}) \in [-s_2, s_2]^2 \\ 0, & otherwise \end{cases}$$

.

The Fourier transform of $D^2_{(m,n)}(x,y)$ is

$$\widehat{D}^2_{(n,m)}(x,y) = FT\left[w_2 1_{[s_2,s_2]^2} * I_R(x,y) - w_2 1_{[s_2,s_2]^2} * I_R\left(x+(m-a), y+(n-a)\right)\right]$$

$$= FT\left[w_2 1_{[s_2,s_2]^2} * \left(I_R(x,y) - I_R\big(x+(m-a), y+(n-a)\big)\right)\right]$$

$$= FT\big[w_2 1_{[s_2,s_2]^2}\big] FT\left[I_R(x,y) - I_R(x+(m-a), y+(n-a))\right] \quad (18)$$

Substitute (10) into (14), we get

$$\widehat{D}^2_{(n,m)}(x,y) = FT\big[w_2 1_{[s_2,s_2]^2}\big]\widehat{D}^1_{(p,q)}(x,y)$$

$$= \left(\sum_{k=-\infty}^{\infty}\sum_{l=-\infty}^{\infty} w_2(k,l) 1_{[s_2,s_2]^2}(k,l) e^{-i2(kp+lq)}\right)\widehat{D}^1_{(n,m)}(x,y) \quad (19)$$

Hence, from equation (19), we can obtain

$$\left|\widehat{D}^2_{(n,m)}(x,y)\right| = \left|\sum_{k=-s_2}^{s_2}\sum_{l=-s_2}^{s_2} \frac{e^{-\left(\frac{k^2+l^2}{2\sigma_2{}^2}\right)}}{\sum_{k'=-s_2}^{s_2}\sum_{l'=-s_2}^{s_2} e^{-\left(\frac{k'^2+l'^2}{2\sigma_2{}^2}\right)}} e^{-i2(kn+lm)}\, \widehat{D}^1_{(n,m)}(x,y)\right|$$

$$=$$

$$\leq \sum_{k=-s_2}^{s_2}\sum_{l=-s_2}^{s_2} \left|\frac{e^{-\left(\frac{k^2+l^2}{2\sigma_2{}^2}\right)}}{\sum_{k'=-s_2}^{s_2}\sum_{l'=-s_2}^{s_2} e^{-\left(\frac{k'^2+l'^2}{2\sigma_2{}^2}\right)}}\right| \left|\widehat{D}^1_{(n,m)}(x,y)\right| \leq \left|\widehat{D}^1_{(n,m)}(x,y)\right| \quad (20)$$

On the other hand, from equation (13) and Plancherel-Parseval's theorem, we have

$$r_2(x,y) = \sum_{m=0}^{2a}\sum_{n=0}^{2a}\left|D^2_{(m,n)}(x,y)\right|^2 = \frac{1}{(2a+1)^2}\sum_{m=0}^{2a}\sum_{n=0}^{2a}\left|\widehat{D}^2_{(n,m)}(x,y)\right|^2$$

From (16), we get

$$r_2(x,y) \leq \frac{1}{(2a+1)^2}\sum_{m=0}^{2a}\sum_{n=0}^{2a}\left|\widehat{D}^1_{(p,q)}(x,y)\right|^2 \leq \sum_{m=0}^{2a}\sum_{n=0}^{2a}\left|\widehat{D}^1_{(m,n)}(x,y)\right|^2$$

$$r_2(x,y) \leq r_1(x,y)$$

This proves that the local variability in blurred part is smaller than local variability in focused part.

AUTHORS

Rachid Sabre received the PhD degree in statistics from the University of Rouen, Rouen, France, in 1993 and Habilitation (HdR) from the University of Burgundy, Dijon, France, in 2003.He joined Agrosup Dijon, Dijon, France, in 1995, where he is an Associate Professor. From 1998 through 2010, he served as a member of "Institut de Mathématiques de Bourgogne", France. He was a member of the Scientific Council AgroSup Dijon from 2009 to 2013. In 2012, he has been a member of " Laboratoire Electronique, Informatique, et Image" (Le2i), France. Since 2019 has been a member of Laboratory Biogeosciences UMR CNRS, University of Burgundy. He is author/co-author of numerous papers in scientific and technical journals and conference proceedings. His research interests lie in areas of statistical process and spectral analysis for signal and image processing.

Ias Sri Wahyuni was born in Jakarta, Indonesia, in 1986. She earned the B.Sc. and M.Sc. degrees in mathematics from the University of Indonesia, Depok, Indonesia, in 2008 and 2011, respectively.In 2009, she joined the Department of Informatics (COMPUTING) System, Gunadarma University, Depok, Indonesia, as a Lecturer. She is currently a PhD student at University of Burgundy, Dijon, France. Her current research interests include statistics and image processing.